Journal of Computational Methods in Molecular Design, *2018, 8 (1):1-12*

ISSN : 2231- 3176
CODEN (USA): JCMMD

Computational Study on Conducting Polymers of Thieno [3,4-b] Pyrazines and Its Derivatives

Wasihun Menberu[1]*, Ahmed Mustefa[2]

[1]School of Chemistry and Chemical Engineering, University of the Chinese Academy of Sciences, Beijing 100049, People's Republic of China

[2]Addis Ababa University, College of Natural and Computational Sciences, Department of Chemistry, Addis Ababa, Ethiopia

---

ABSTRACT

In this work, the geometrical and electronic properties of thieno[3,4-b]pyrazine (TP) based donor-acceptor conjugated oligomers were studied by density functional theory (DFT) at the B3LYP level with 6-31G (d,p) basis set. The inter-rings bonds are longer than normal double bonds but shorter than the single bonds; these indicate that the emerging of a quinoidal likes distortions as a result of oxidation. The absorption spectra of polymers were studied using the TDDFT/B3LYP/6-31G. Two main absorption peaks can be seen; the one largest in wavelength corresponding to a HOMO to LUMO transition, the result obtained from thermodynamic properties showed that all the studied compounds have almost similar properties.

Keywords: Thieno[3,4-b]pyrazine, Donor-acceptor, Low-band gap, Optoelectronic, DFT, Geometrical and electronic properties

---

INTRODUCTION

Polymers are macromolecules built up by the linking of large number of much smaller molecules. The smaller molecules that combine with each other to form polymer molecule are termed monomers, and the reactions by which they combine are termed polymerization [1].

Intrinsically conducting polymers (ICPs) are an exciting new class of electronic materials, which have attracted rapidly increasing interest since their discovery in 1979 [2]. ICPs have the potential of combining the high conductivities of pure metals with the processibility, corrosion resistance, and low density of polymers [3]. Additionally, they have many applications in the fields of rechargeable batteries [4,5], electro chromic display devices [5,6], electromagnetic shielding [7], sensor technology [8], non-linear optics [9] and molecular electronics [10,11].

The motivation of this manuscript paper is attempting to find an organic polymer that would be a "metal" or that would at least have a partial metallic character; a lot of studies have been done for about more than 30 years. From the early days of study of conducting polymers scientists envisaged that there might be a class of these polymers, that would have either a zero band gap (a single and continuous band consisting of the valence and conduction bands) or a very low band gap.

In material science, band structure engineering has become important since the band gap (Eg) is one of the most important factors for controlling the optical and electronic properties of conducting polymer. Especially the design of low band gap polymers (Eg<1.0 eV) is a major challenge in the field of conducting polymers now a day fused ring system containing compounds is better approach to solve the problem. Based on computational modeling we try to calculate the band gap and other properties.

Polyheterocycles as conducting polymers

The current interest in conductive polymers began in the 1970's, when it was found that the electrical conductivity of polyacetylene, a semi-conductor when pristine, could be increased by over fifteen orders of magnitude by treatment with oxidizing agents such as iodine. The synthesis of polyacetylene in the highly conducting doped form was a starting point for a considerable number of studies. Electrodeposition of free standing films of polypyrrole from organic media [12] opened the way to intensive research into polyheterocyclic and polyaromatic conducting polymers [13]. The electrochemical oxidation of these resonance-stabilized aromatic molecules has become one of the principal methods for preparing the conjugated, electronically conducting polymers.

Band gap engineering of π-conjugated polymers

The energy difference between valence and conduction bands in conducting materials (including conductive polymers) is analogous to the HOMO (Highest Occupied Molecular Orbital)-LUMO (Lowest Unoccupied Molecular Orbitals) gap of small molecules, generally referred to as the energy gap (Eg) [14].

The HOMO-LUMO gap is a very important parameter in defining the optical and electronic properties of materials. When a molecule absorbs energy; the electron gets promoted from an occupied molecular orbital to a vacant molecular orbital at a higher energy. The lowest energy electronic transition is from HOMO to LUMO, however other transitions can occur, including $\sigma \rightarrow \sigma^*$, $\sigma \rightarrow \pi^*$, $n \rightarrow \sigma^*$, $n \rightarrow \pi^*$ and additional $\pi \rightarrow \pi^*$ transitions .

The energy difference between the HOMO and LUMO decreases as conjugation is extended due to relative energies of the increasing number of conjugated π-orbitals (Figure 1).

The conductivity of a π-conjugated system is directly dependent on the energy gap; the smaller the energy gap, the greater the conductivity [15]. Insulators, such as diamond have an energy gap of 5.5 eV, while a semiconductor material such as silicon has 1.1 eV [16]. While the energy gap of any metal will be ≈ 0 eV due to the overlap of the conduction and the valence bands. Conjugation needs to extend over the length of the entire molecule in order to obtain the narrowest possible energy gap. The energy gap (Eg) of these linear π-conjugated systems can be influenced by the sum of five structural contributors:

$$Eg = E_{BLA} + E_{Res} + E_{sub} + E_{\theta} + E_{Int}$$

where BLA represents the bond length alteration; Res, resonance; Sub, the effect of substituent; θ, for dihedral angle; and Int, intermolecular interactions [17].

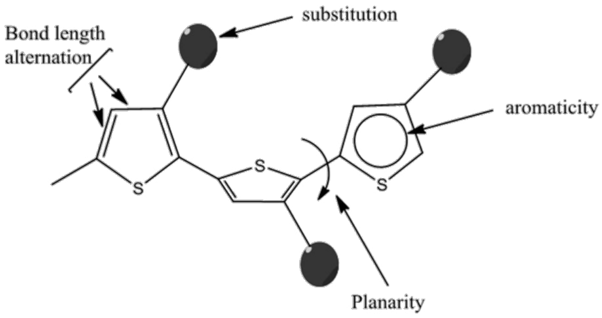

Figure 1: Structural factors that affect the HOMO-LUMO gap of linear π-conjugated systems

E_{Res} confines the delocalization of π-electrons within the aromatic ring while the E_{θ} between the consecutive units limit the π-electrons along the conjugated backbone. The E_{sub} directly modulates the energy levels based on the electron withdrawing or donating substituents. When individual molecules or polymer chains are assembled into a material, the E_{Int} can affect the magnitude of the molecules of the energy gap because each polymer chain experiences weak intermolecular interaction. Therefore, the five energy gap influencers of E_{BLA}, E_{Res}, E_{Sub}, E_{θ}, and E_{Int} are essential parameters to synthetic approaches for conjugated polymer synthesis [17].

Further reduction in band gap is possible by enhancing the strength of donor and acceptor moieties *via* strong orbital interactions. In donor-acceptor systems, the introduction of electron withdrawing groups reduces Eg by lowering the LUMO levels whereas, the introduction of electron donating groups reduces Eg by raising the HOMO levels.

Therefore, designing of extremely low Eg polymers requires strong donors and acceptors. The synthetic principles for lowering the band gap of linear π-conjugated polymers have been reviewed by Roncali [17].

COMPUTATIONAL METHODS

All calculations were done by using Gaussian09W [18]. The geometries of the thieno[3,4-b]pyrazines and its derivatives were optimized at by Becke's three parameter hybrid functional for exchange combined with the correlation functional due to Odian [1], Frisch [18] and Foresman and Frisch [19] level using first 3-21G* basis set and further re-optimized using 6-31G(d,p) basis set. DFT/B3LYP/6-31G (d,p) has been found to be an accurate formalism for calculating the geometrical, electronic structures and optical properties of many organic molecules [20-22].

All the optimizations were done without constraint on dihedral angles. The HOMO, LUMO and band gap (HOMO-LUMO) energies were also deduced for the stable structures.

In the UV-Vis electronic transitions, calculations of excited states were performed using the Time-Dependent Density Functional Theory (TDDFT) with B3LYP/6-31G (d,p) in CCl_4 solvent formalism as implemented in the Gaussian09 code because of the nonelectrolyte nature, Transparency and nonpolar Character of molecules (i.e., CCl_4) that incapability to form ions at under normal Condition

All the calculations were performed at 298.15 K and 1.00 Atm. This project was done using the Intel [R] core(TM) 2 duo CPU Version 2002 computer.

Compounds investigated

Thieno[3,4-b]pyrazine, [TP] a promising material for optoelectronic devices. Thieno[3,4-b]pyrazines have been shown to be excellent precursors for the production of low band gap conjugated polymers [23-26]. Recently, photovoltaic devices consisting of thieno[3,4-b]pyrazines based low-band gap polymers as hole-transporting materials have shown improved efficiencies. The optimized structures of the studied compounds have been shown in Figure 2.

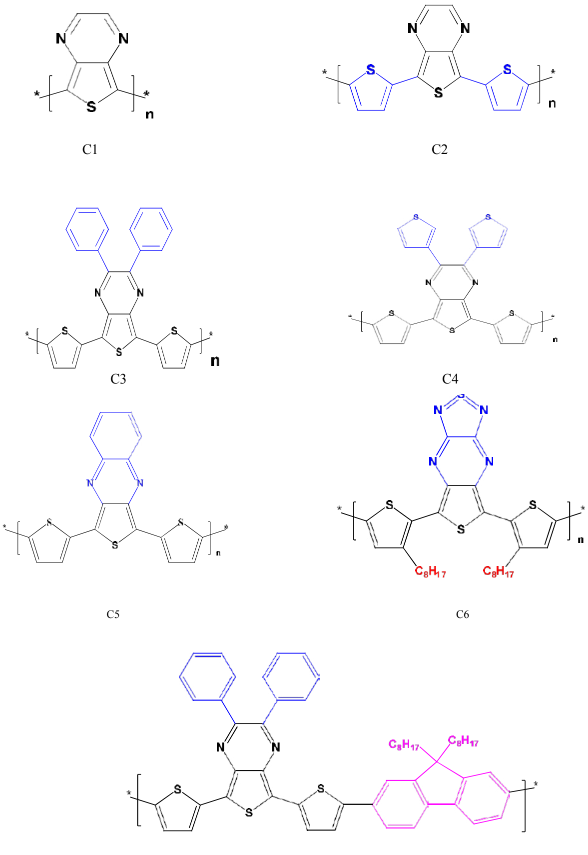

C1 C2 C3 C4 C5 C6 C7

Figure 2: Structures of the investigated compounds

RESULTS AND DISCUSSION

Geometry optimization

For determining the optimization of the studied compounds the atom labeling of thieno[3,4-b]pyrazines and its derivatives are given in Figure 3.

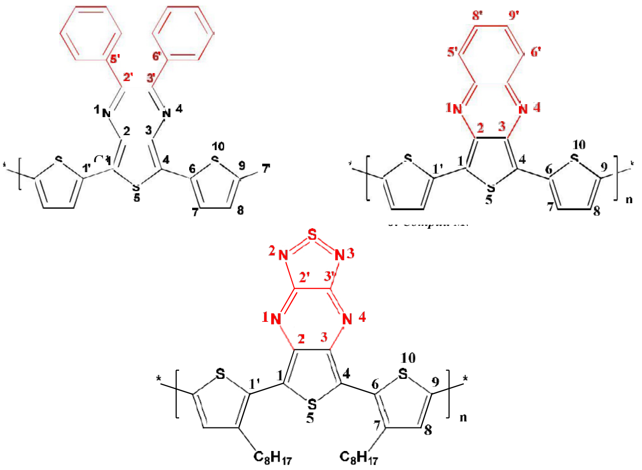

Figure 3: The atom labeling of investigated compounds

The calculated structural parameters are given in Tables 1 and 2. It is observed that upon the removal of an electron from the neutral compounds the bond lengths of the oligommers changed. Single bonds become shorter and double bonds become longer in the oxidized structures than the reduced (neutral) structures. This shows that upon oxidation the single bonds show double bond character and the double bonds show single bond character and this implies the emerging of quinoid character of the oligommers.

In all compounds the bond length between $C_{1'}$-C_1, C_2-C_3 and C_4-C_6 [for example in compound C2 (1.4390 to 1.4066 Å), (1.4435 to 1.4178 Å) and (1.439 to 1.4066 Å)] decrease upon removal of an electron, which indicate that the formation of quinoid character upon oxidation.

In all compounds the inter-rings bonds are longer than normal double bonds but shorter than the single bonds. From these bond lengths it is also possible to confirm the emerging of a quinoidal like distortions as a result of oxidation.

Based on the above results Figure 4 explains the formation of quinoidal structures from the aromatic structures [27].

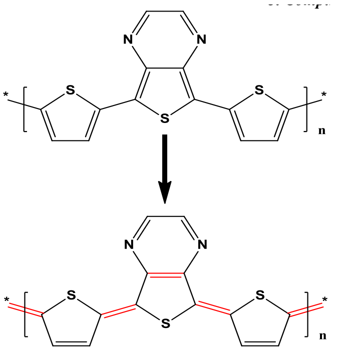

Figure 4: Structure of aromatic and quinoid forms of the terthienyl TP

The C2'-C3' bonds in compounds (C3), (C4) and (C7) increase compared to other compounds.

Due to the steric hindrance between the phenyl and thiophene groups to thieno [3,4-b] pyrazine.

In thieno [3,4-b] pyrazine the adjacent C-S bond length are identical in the reduced form, and this result also observed for the oxidized form since they are in identical chemical environments. While the extreme C-S bond of unsubstituted thiophene is not identical. For example, in compound C2 the bond lengths between $S_{10}C_6$ and C_9S_{10} are 1.7609 and

1.7331 Å, respectively which shows that they are not identical even if they are in the same environment, due to the steric effect of pyrazine.

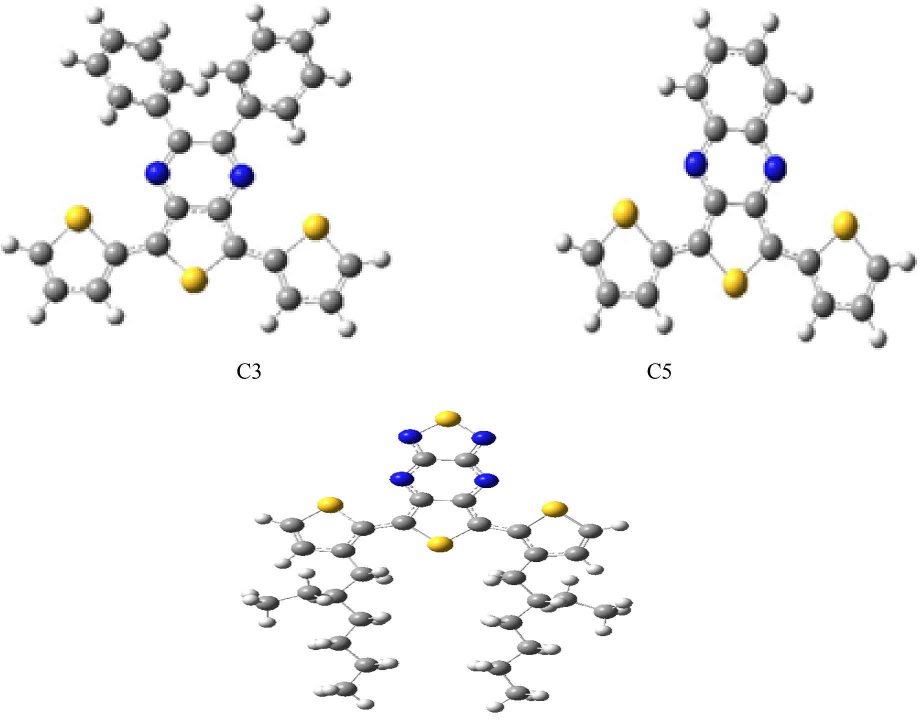
C3 C5

C6

Figure 5: Optimized geometries obtained by B3LYP/6-31G (d,p) of the selected molecule

Table 1: Optimized selected bond lengths (in Å) of the studied molecules in neutral (reduced) and polaronic (oxidized) states obtained by B3LYP/6-31G (d,p) level

Parameter	**C1**		**C2**		**C3**		**C4**	
	Red	**Oxd**	**Red**	**Oxd**	**Red**	**Oxd**	**Red**	**Oxd**
C_1'C_1	-	-	1.4390	1.4066	1.4384	1.4084	1.4385	1.4088
C_1C_2	1.3835	1.4214	1.3978	1.4294	1.3975	1.4258	1.3969	1.4248
C_2C_3	1.4525	1.4233	1.4435	1.4178	1.4367	1.4137	1.4365	1.4144
C_3C_4	1.3835	1.4214	1.3978	1.4294	1.3975	1.4258	1.3969	1.4248
C_4S_5	1.7177	1.7276	1.7468	1.7543	1.7489	1.7579	1.7495	1.7586
S_5C_1	1.7177	1.7276	1.7468	1.7543	1.7489	1.7579	1.7495	1.7586
C_2N_1	1.3723	1.3455	1.3643	1.3494	1.3583	1.3441	1.3584	1.3445
N_1C_2'	1.3092	1.3301	1.3116	1.3217	1.3182	1.3302	1.3185	1.3309
C_2'C_3'	1.4412	1.4272	1.4358	1.4260	1.4701	1.4671	1.4716	1.4689
C_3'N_4	1.3092	1.3301	1.3116	1.3217	1.3182	1.3302	1.3185	1.3309
N_4C_3	1.3723	1.3455	1.3643	1.3494	1.3583	1.3441	1.3584	1.3445
C_2'C_5'	-	-	-	-	1.4888	1.4791	1.4799	1.4678
C_3'C_6'	-	-	-	-	1.4888	1.4791	1.4799	1.4678
C_4C_6	-	-	1.439	1.4066	1.4384	1.4084	1.4385	1.4088
C_6C_7	-	-	1.3846	1.4081	1.3845	1.4055	1.3844	1.4052
C_7C_8	-	-	1.4185	1.3975	1.4188	1.4	1.4189	1.4004
C_8C_9	-	-	1.3695	1.3866	1.3693	1.3841	1.3692	1.3837
C_9S_{10}	-	-	1.7331	1.7176	1.7336	1.7202	1.7337	1.7206
$S_{10}C_6$	-	-	1.7609	1.7692	1.7613	1.7678	1.7612	1.7673

Table 2: Optimized selected bond lengths (in Å) of the studied molecules in neutral (reduced) and polaronic (oxidized) states obtained by B3LYP/6-31G (d,p) level

Parameter	C5		C6		C7	
	Red	Oxd	Red	Oxd	Red	Oxd
$C_1{'}C_1$	1.4362	1.407	1.4394	1.4068	1.4378	1.4157
C_1C_2	1.4073	1.4337	1.4180	1.4441	1.3978	1.4212
C_2C_3	1.4540	1.4348	1.4753	1.4528	1.4361	1.4167
C_3C_4	1.4073	1.4337	1.4180	1.4441	1.3994	1.4227
C_4S_5	1.7407	1.7519	1.7396	1.7544	1.7502	1.7613
S_5C_1	1.7407	1.7519	1.7396	1.7544	1.75	1.7536
C_2N_1	1.3444	1.3295	1.3362	1.3236	1.3584	1.347
$N_1C_2{'}$	1.3354	1.3466	1.3364	1.345	1.3185	1.3277
$C_2{'}N_2$	-	-	1.3508	1.3426	-	-
N_2S_1	-	-	1.6308	1.6327	-	-
S_1N_3	-	-	1.6308	1.6327	-	-
$N_3C_3{'}$	-	-	1.3508	1.3426	-	-
$C_{2'}C_{3'}$	1.4601	1.4577	1.4677	1.462	1.4694	1.4646
$C_3{'}N_4$	1.3354	1.3466	1.3364	1.345	1.3188	1.3289
N_4C_3	1.3444	1.3295	1.3362	1.3236	1.357	1.3459
$C_2{'}C_5{'}$	1.4326	1.423	-	-	1.4889	1.4826
$C_3{'}C_6{'}$	1.4326	1.423	-	-	1.4888	1.4823
$C_5{'}C_8{'}$	1.3661	1.3721	-	-	-	-
$C_8{'}C_9{'}$	1.4332	1.427	-	-	-	-
$C_9{'}C_6{'}$	1.3661	1.3721	-	-	-	-
C_4C_6	1.4362	1.407	1.4394	1.4068	1.4342	1.402
C_6C_7	1.3861	1.4068	1.4021	1.4301	1.3867	1.4112
C_7C_8	1.4178	1.3991	1.4249	1.4064	1.4112	1.3845
C_8C_9	1.3699	1.3847	1.3670	1.3795	1.3816	1.4075
C_9S_{10}	1.7334	1.7195	1.7251	1.7141	1.7546	1.7551
$S_{10}C_6$	1.7619	1.7681	1.7696	1.7793	1.7593	1.7638
$C_9C_7{'}$	-	-	-	-	1.4633	1.441

Table 3: Selected bond length (in Å) of the studied molecules in neutral (reduced) state calculated in this work is listed with earlier theoretical and experimental results reported in literatures

Parameter	C1		(Exp)a [28-30]	C2	
	This work (B3LYP/6-31G (d,p)	Cal. [31] B3LYP cc-pVDZ		This work (B3LYP/6-31G (d,p)	Cal [31] B3P86-30% functional CEP-31G*
C_1C_2	1.3835	1.387	1.371	1.3978	1.412
C_2C_3	1.4525	1.453	1.432	1.4435	1.449
C_3C_4	1.3835	1.387	1.371	1.3978	1.412
C_4S_5	1.7177	1.722	1.692	1.7468	1.743
S_5C_1	1.7177	1.722	1.692	1.7468	1.743
C_2N_1	1.3723	1.373	1.374	1.3643	1.365
$N_1C_2{'}$	1.3092	1.311	1.305	1.3116	1.312
$C_2{'}C_3{'}$	1.4412	1.443	1.464	1.4358	1.453
$C_3{'}N_4$	1.3092	1.311	1.305	1.3116	1.312
N_4C_3	1.3723	1.373	1.374	1.3643	1.365
C_4C_6	-	-	-	1.439	1.448
C_6C_7	-	-	-	1.3846	1.402
C_7C_8	-	-	-	1.4185	1.421
C_8C_9	-	-	-	1.3695	1.402
C_9S_{10}	-	-	-	1.7331	1.754
$S_{10}C_6$	-	-	-	1.7609	1.754

X-ray data averaged from the structures reported for 2,3-dimethyl -TP [28], 2,3 dihexyl - TP [29] and 2,3-bis(bromomethyl) -TP [30].

Considering C-C, C-N and C-S bond lengths for compound **C1** and **C2**, methods used in this work estimated a satisfactory result with the experimental but the theoretical result reported using B3LYP cc-pVDZ and B3P86-30% functional CEP-31G* are slightly different from the experimental results (Tables 3 and 4).

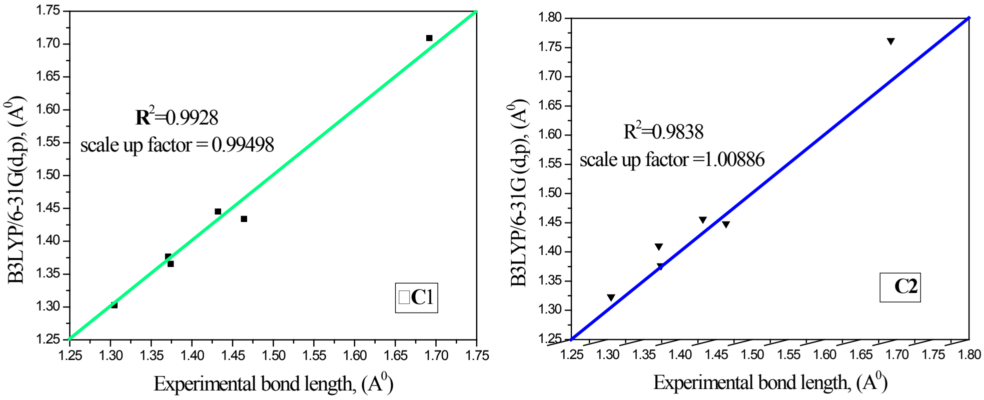

(a) (b)

Figure 6: Correlation graph between the calculated *verses* the experimental a) for compound **C1** and b) for compound **C2**

Figure 6 shows the correlation between experimental and theoretical bond length in (A^0). The correlation values are found to be 0.9928 and 0.9838 for compound C1 and C2, respectively. The scaled linear regression data for compound C1 and C2 which shows that there was good correlation between the experimental bond length and the computational.

For a compound C6 the adjacent C-N and N-S bond lengths are identical in the reduced form, and this result is also observed for the oxidized form since they are in identical chemical environments. Both N_2-S_1 and S_1-N_3 bond length in compound C6 increase up on the removal of an electron, from 1.6308 Å to 1.6327 Å, while the bond length C_2’-N_2 and N_3-C_3’ decrease up on the removal of an electron, from 1.3508 Å to 1.3426 Å up on the removal of electron the bond length is changed this is due to the contribution of hetro atom to the resonance of aromatic ring. In compound C6 the bond length between N_1-C_2’ and C_2’-C_3’ (1.3364 Å, 1.4677Å), respectively increased with compare to compound C2 (1.3116 Å, 1.4358Å), respectively due to introduction of fused thiadiazol to Thieno[3,4-b]pyrazine. The bond length between C_1’-C_1, C_2-C_3 and C_4-C_6 in compound C6 (1.4394 to 1.4068 Å), (1.4753 to 1.4528 Å) and (1.4394 to 1.4068 Å)] decrease up on the removal of an electron, which indicate that the formation of quinoid character up on oxidation.

Comparison of C5 and C6 show that the bond length between C_2’-N_2 (1.3508 Å) and C_2’-C_5’ (1.4326 Å), respectively increase due to steric effect of (N-H) in compound C5.

According to previous work using AM_1 method on the tetramer models of [1,2,5]thiadiazolo[3,4-b]thieno[3,4-e] pyrazine with thiophene (C6), s-trans coplanar structures are, in fact, most stable in energy [27]. Similar systems involving thieno[3,4-b]pyrazine also have nearly coplanar X-ray structures [27]. This is due to the favorable inter-ring S-N or H-N interactions, where the nitrogen atoms in the pyrazine ring are important to retain the coplanarity. We therefore consider that the coplanar s-trans geometries are reasonable for the one-dimensional systems as in Figure 5.

Table 4: Selected bond length (in Å) of the studied molecules (**C6**) in neutral (reduced) and polaronic (oxidized) states

Parameter	**C6**		
	This work (B3LYP/6-31G (d, p) Neutral form	**This work (B3LYP/6-31G (d, p) Polaronic form**	**Cal [16] MNDO/PM3 Neutral form**
$C_{1'}C_1$	1.4394	1.4068	-
C_1C_2	1.4180	1.4441	1.428
C_2C_3	1.4753	1.4528	1.470
C_3C_4	1.4180	1.4441	1.428
C_4S_5	1.7396	1.7544	1.697
S_5C_1	1.7396	1.7544	1.697
C_2N_1	1.3362	1.3236	1.344
$N_1C_{2'}$	1.3364	1.345	1.376

$C_{2'}N_2$	1.3508	1.3426	1.352
N_2S_1	1.6308	1.6327	1.702
S_1N_3	1.6308	1.6327	1.702
$N_3C_{3'}$	1.3508	1.3426	1.352
$C_{2'}C_{3'}$	1.4677	1.462	1.470
$C_{3'}N_4$	1.3364	1.345	1.376
N_4C_3	1.3362	1.3236	1.344
C_4C_6	1.4394	1.4068	1.434
C_6C_7	1.4021	1.4301	1.381
C_7C_8	1.4249	1.4064	1.423
C_8C_9	1.3670	1.3795	1.381
C_9S_{10}	1.7251	1.7141	1.739
$S_{10}C_6$	1.7696	1.7793	1.739

UV-visible absorption

The electronic spectra involving transition of valence electrons that occur in the UV-Vis region were studied computationally in order to investigate the optical property and electronic transition. The excitation energy and UV-Vis absorption spectra for the singlet-singlet transition of all compounds were simulated using TD-DFT with B3LYP functional in chloroform solution.

The calculated absorption λ_{max} (nm) and oscillator strength (O.S) along with main excitation configuration of the studied compounds are shown in Table 5.

Table 5: Absorption wavelength λ_{abs} (nm), excitation energies and oscillator strengths obtained by the TD-DFT method

Compound	Excitation States	λ_{abs} (nm)	E_{ex} (nm)	O.S (f) a.u	MO/character	Coefficient
C1	1	377.09	377.14	0.0029	HOMO-1→ LUMO	0.70470
	2	359.31	359.35	0.0437	HOMO→ LUMO	0.69637
	3	279.41	279.44	0.2562	HOMO-3→ LUMO	0.66901
C2	1	614.09	614.16	0.3288	HOMO→ LUMO	0.70177
	2	390.35	390.40	0.0016	HOMO-4→ LUMO	0.69755
	3	362.53	362.57	0.0133	HOMO-1→ LUMO	0.65900
C3	1	623.67	623.74	0.2581	HOMO→ LUMO	0.70240
	2	408.51	408.56	0.1972	HOMO-1→ LUMO	0.65921
	3	393.66	393.71	0.0016	HOMO-3→ LUMO	0.67587
C4	1	618.94	619.00	0.2600	HOMO→ LUMO	0.70238
	2	431.24	431.28	0.1969	HOMO-1→ LUMO	0.66351
	3	389.49	389.53	0.0016	HOMO-4→ LUMO	0.56614
C5	1	830.81	830.93	0.1924	HOMO→ LUMO	0.70710
	2	443.16	443.22	0.0009	HOMO-4→ LUMO	0.70205
	3	406.21	406.26	0.0593	HOMO-1→ LUMO	0.67724
C6	1	1509.74	1509.9	0.0613	HOMO→ LUMO	0.71620
	2	521.63	521.70	0.0004	HOMO-4→ LUMO	0.59176
	3	494.42	494.49	0.0520	HOMO-1→ LUMO	0.59953
C7	1	684.52	684.62	0.5498	HOMO→ LUMO	0.70408
	2	454.95	455.01	0.0506	HOMO-1→ LUMO	0.68089
	3	424.88	424.93	0.7716	HOMO→ LUMO+1	0.69345

From Table 5, compounds C2, C3, C4 and C7 exhibit a strong absorption band in the visible region around 614-684 nm, and for the compound C5 and C6 they are out of UV-VIS region due to the fused system and the hetero atom effect.

From Table 5 it is clear that the compound C1 is absorbing at a shorter wavelength range and it must be colorless, while other compounds except C5 and C6 the absorption wavelength increases to the visible range, which indicates they are colored.

With increase in the chain length, the excitation energy decreases, implying ease of removing electrons upon polymerization. In compounds C5 and C6 the excitation energy is very small as compared to others which indicate the ease of removing electrons.

In all compounds two peaks were obtained from lowest singlet electronic excitation is characterized π-π* transition while the long-wavelength absorption peaks can be attributed to intramolecular charge transfer between the thiophene donor and the acceptor moieties (Figure 7).

Excitation state one ($S_0 \longrightarrow S_1$) corresponds almost exclusively to the promotion of an electron from the HOMO to LUMO orbital except compound C1.

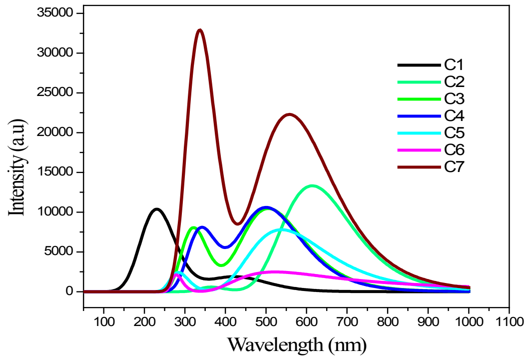

Figure 7: Simulated UV-Vis absorption spectra of the investigated compounds in CCl_4 solvent

The absorption wavelengths arising from ($S_0 \rightarrow S_1$) electronic transition increase progressively with the increase of conjugation lengths (i.e., **C1<C2<C4<C3<C7**) which implies decrease in LUMO and increase in HOMO energy. A good photovoltaic material should have broad and strong visible absorption characteristics.

Band gaps

The band gap is obtained by subtracting the energy of the lowest unoccupied molecular orbital (LUMO) from the energy of the highest occupied molecular orbital (HOMO), i.e., E_{LUMO}-E_{HOMO}.

Table 6: The theoretical electronic properties (HOMO, LUMO and Eg) of thieno[3,4-b]pyrazines and its derivatives calculated by B3LYP/6-31G (d,p)

Compounds	**Neutral form**			**Polaronic form**		
	E_{HOMO} (ev)	**E_{LUMO} (ev)**	**E_g**	**E_{HOMO} (ev)**	**E_{LUMO} (ev)**	**E_g**
C1	-6.2441	-2.2743	3.9698	-12.0283	-8.1363	3.8920
C2	-5.0119	-2.6339	2.3780	-8.9195	-6.6583	2.2612
C3	-4.8927	-2.5511	2.3416	-8.4809	-6.1898	2.2911
C4	-4.9220	-2.5672	2.3548	-8.4819	-6.1779	2.3039
C5	-4.8044	-2.9777	1.8267	-8.5389	-6.7060	1.8328
C6	-4.8236	-3.5780	1.2456	-8.3603	-6.9377	1.4226
C7	-4.7347	-2.5803	2.1544	-7.5778	-5.6325	1.9453

From Table 6 it is observed that the calculated band gap E_g of the studied model compounds increases in the following order **C6<C5<C7<C3<C4<C2<C1**. The much lower E_g of **C5** and **C6** is observed due to the fused ring system and the hetero atom effect.

Adding of aliphatic groups in **C6** and **C7** has insignificant effect on electronic property (band gap) of the compounds. Rather it affects the solubility of the polymer.

For **C6** the three rings in the terthienyl TP units are almost coplanar, which is preferable for the band gap reduction of π-conjugated systems.

In compound three (**C3**) and four (**C4**) the bond length between C1'-C1 have a length of about 1.4384, 1.4385 Å, respectively while the C1-C2 have a length of about 1.3975, 1.3969 Å, respectively Based on these bond distances the bond length alternation (BLA) can be quantified taking $\Delta R_{BLA} = R(C_1{'}C_1) - R(C_1C_2)$ as measures of the BLA take values of 0.0409 and 0.0416 Å, respectively which indicate that compound **C3** has better band gap than compound **C4**.

Table 7: Comparison of experimental band gaps with calculated band gaps at different methods

Band gap (eV) (Neutral form)			
Compounds	**This work (B3LYP/6-31G(d,p)**	**Compounds**	**Cal [32,33]**
C1	3.9698	C1	-
C2	2.3780	C2	1.0[a], 2.369[c]
C3	2.3416	C3 [with alkyl side chain (C_8H_{17})]	1.9[a],1.6[b]
C4	2.3548	C4	1.15[a], 1.4[b]
C5	1.8267	C5	-
C6	1.2456	C6 [without alkyl side chain (C_8H_{17})]	0.30[b]
C7	2.1544	C7	1.6[a],2.0[b]

[a] optical band gap, [b] electrochemical and [c] (B3LYP)/6-31G*

From Table 7 it is observed that the calculated band gap E_g of the studied model compounds compared with experimental band gaps with calculated band gap at (B3LYP)/6-31G Methods in **C2 and C4** the optical band gap and calculated band gap was lower than our calculated results but it was in comparable range however in **C3 and C6** the alkyl side chain may have a big contribution on the band gap of the compounds (Figure 8).

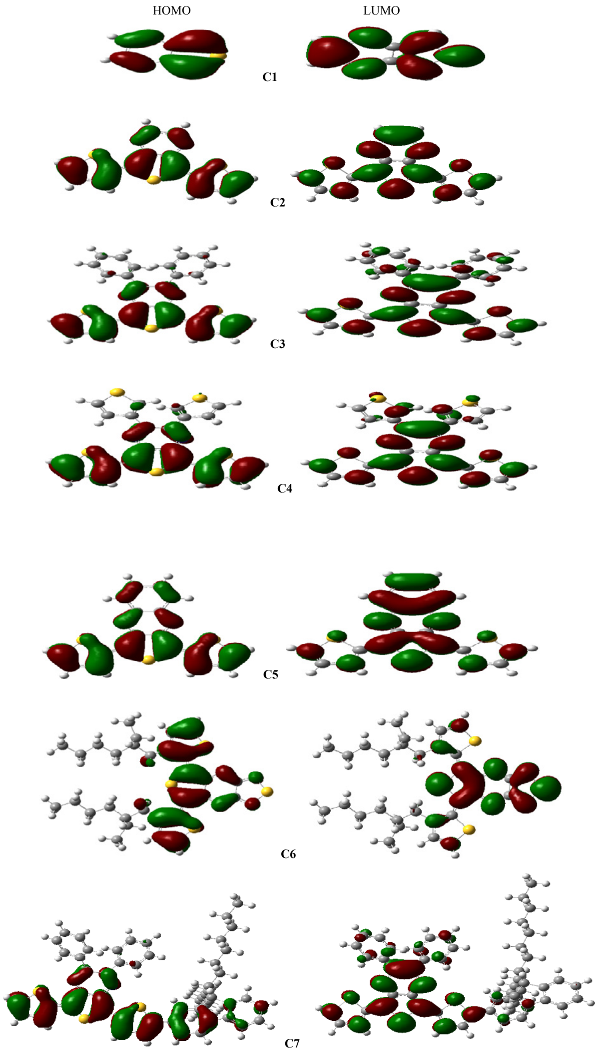

Figure 8: The contour plots of HOMO and LUMO orbital of the studied compounds

Thermodynamic properties

The change in the thermodynamic properties was calculated by subtracting the thermodynamic properties of the reduced compounds from the thermodynamic properties of the oxidized compounds. The results are listed in Table 8.

Table 8: Thermodynamic properties of thieno[3,4-b]pyrazines and its derivatives calculated by B3LYP/6-31G (d,p)

Compounds	$\Delta H^{0}(kcal/mol)$	$\Delta H^{0}(kcal/mol)$	$\Delta S^{0}(cal/mol.K)$
C1	-0.2963	-0.2983	-2.547
C2	-0.231	-0.231	0.417
C3	-0.222	-0.221	0.47
C4	-0.222	-0.222	0.364
C5	-0.221	-0.221	0.224
C6	-0.219	-0.218	2.555
C7	-	-	-

The result shows that all the studied compounds have almost similar change in thermodynamic properties except compound C1 which indicates that upon polymerization the change in thermodynamic properties decreases. This decrease in change in thermodynamic properties shows that the oxidized forms of the compound (C1) is unstable compared to other compounds.

The conjugation length increases the stability of the oxidized species for all cases. For example compound two (C2) has a change in Gibbs free energy of -0.231 kcal/mol, which is less than compound one (C1) with a change in Gibbs free energy of -0.2963 kcal/mol that supports the stability of the radical cation of compound (C2).

CONCLUSION

In this study, theoretical analysis on the geometries and electronic properties of seven compounds that are based on Thieno [3,4-b]pyrazines were studied in order to explain the effect of substituted groups a on the structural and optoelectronic properties of these materials.

The following conclusions were drawn:

- For all studied compounds during oxidation process the single bonds become shorter while multiple ones become longer. The inter ring bonds are longer than normal double bonds. This confirms the emerging of a quinoidal like distortions as a result of oxidation.

- The results of the optimized structures for all studied compounds showed that they have similar conformations except compound C5 and C6.

- The HOMO level, LUMO level, and band gap of the studied compounds were well controlled by the acceptor strength. The calculated band gap (E_{gap}) of the studied molecules was in the range of 1.2456 - 3.9698 eV.

- Compound C5 and C6 have better band gap but the absorption wave length is out of UV-Vis region due to fused system and hetero atom effects.

- The band gap ($E_{g)}$ of the studied model compounds compared with experimental band gaps with calculated band gap at (B3LYP)/6-31G Methods in C2 and C4 the optical band gap and calculated band gap was lower than our calculated results but it was in comparable range

- The UV-Vis absorption properties have been obtained by using TD/B3LYP calculations. The obtained absorption maximums are in the range of 614-684 nm for compounds C2, C3, C4 and C7 as results.

- The result obtained from thermodynamic properties showed that all the studied compounds have almost similar properties except compound one (C1).

The theoretical results suggest that both the acceptor strength and the stable geometry contribute significantly to the electronic properties of alternating donor – acceptor conjugated copolymers.

REFERENCES

[1] Odian, G., 3rd ed, Wiley-Interscience Publication, **1993**, p.1.

[2] Diaz, A.F., Kanazawa, K.K. and Gardini, G.P., *J Chem Soc Chem Commun*, **1979**. p. 635.

[3] Hepburn, A.R., Maud J.M. and Marshall, J.M., *Met Mater (Inst Mater)*, **1991.** 7: p. 747.

[4] Santhanam K.S.V and Gupta, N., *TRIP*, **1993**. 1: p. 284.

[5] Mastragostino, M., et al., *Synth Met*, **1989**. 28: p. 501.

[6] Panero, S., Passerini, S. and Scrosati, B., *Mol Cryst Liq Cryst*, **1993.** 229: p. 97.

[7] Dubois, J.C., *Synth Met*, **1989** 28: p.871.

[8] Roncali, J., et al., *J Chem Soc Chem Commun*, **1989** p. 679.

[9] Salaneck, W.R., Proceedings of the 6th Euro physics industrial workshop, Adam Hilger. **1991**.

[10] Bradley, D.D.C., *Chem Ber*, **1991**. 8: p. 719

[11] Davidson, K., *Educ Chem*, **1991**. 28: p. 155.

[12] Diaz, A.F., *J Electrochem Soc*, **1989**. 123: p. 115.

[13] Waltman, R.J., *Can J Chem*, **1986**. 64: p. 76.

[14] Hissler, M., Dyer, P. and Reau, R., *Coord Chem Rev*, **2003**. 244: p. 1

[15] Yamamoto, T.J., *J Chem Soc Chem Commun*, **1981**. p. 187.

[16] Streetman, B. and Banerjee, S., 6th ed. NJ: Prentice Hall, **2000**.

[17] Roncali, J., *Macromol Rapid Commun*, **2007**. 28: p. 1761.

[18] Frisch, M.J., GAUSSIAN 09, Revision B.04, Gaussian, Inc., Pittsburgh PA, **2003**.

[19] Foresman, J.B. and Frisch, E., Gaussian Inc.: Pittsburgh, **1993**.

[20] Liu, T., *Polymer*, **2007**. 48: p. 502.

[21] Yang, L., *Polymer*, **2006**, 47: p. 1397.

[22] Zhao, G.J., *J Phys Chem C*, **2009**. 113: p. 2636.

[23] Zhang, F., *Adv Funct Mater*, **2005**, 15: p.745.

[24] Wienk, M.M., *J Appl Phys Lett*, **2006.** 88: p. 153511.

[25] Wang, X., *Adv Funct Mater*, **2005**. 15: p. 1665.

[26] Thomas, K.R.J., *Adv Mater*, **2002.** 14: p. 822.

[27] Tachibana, M., *J Phys Chem B*, **2002**. 106: p. 3549.

[28] Kenning, D.D., *J Org Chem*, **2002.** 67: p. 9073.

[29] Wen, L., *Macromolecules*, **2008**. 41: p. 4576.

[30] Wen, L., *J Org Chem*, **2008**. 73: p. 8529.

[31] Kitamura, C., Tanaka, S. and Yamashita, Y., *J Chem Soc Chem Commun*, **1994**. p. 1585.

[32] Santhanam, K.S.V. and Gupta, N., *TRIP*, **1993**. 1: p. 284.

[33] Mastragostino, M., *Synth Met*, **1989**. 28: p. 5